Journal of Applied Polymer Science

Properties of Poly(lactic acid) and Poly(ethylene oxide) Solvent Polymer Mixtures and Nanofibers Made by Solution Blow Spinning

Juliano E. Oliveira,[1,2] Eduardo A. Moraes,[2] José M. Marconcini,[2] Luiz H. C. Mattoso,[2] Gregory M. Glenn,[2,3] Eliton S. Medeiros[4]

[1]Programa de Pós-Graduação em Ciência e Engenharia de Materiais, Departamento de Engenharia de Materiais, Universidade Federal de São Carlos, Rodovia Washington Luis, km 235 Monjolinho, 13.565-905, São Carlos, São Paulo, Brazil

[2]Laboratório Nacional de Nanotecnologia para o Agronegócio, Embrapa Instrumentação Agropecuária, Rua XV de Novembro, 1452 Centro, 13.560-970 São Carlos, São Paulo, Brazil

[3]Bioproduct Chemistry and Engineering, Western Regional Research Center, United States Department of Agriculture, Agricultural Research Service, Albany, California 94710

[4]Departamento de Engenharia de Materiais, Universidade Federal da Paraíba, Cidade Universitária, 58.051-900, João Pessoa, Paraíba, Brazil

Correspondence to: E. S. Medeiros (E-mail: eliton@ct.ufpb.br, eliton_s@yahoo.com)

ABSTRACT: The properties of mixtures of poly(lactic acid) (PLA) and poly(ethylene oxide) (PEO) were studied in polymer solutions by dilute solution viscometry, and in-solution blow-spun nanofibers were studied by microscopy (scanning electron and transmission electron microscopy) and thermal and spectral analysis. Three mixtures of PLA and PEO (3:1, 1:1, and 1:3) were solution-blended in chloroform. Dilute solvent viscometry indicated that the 3:1 mixture of PLA and PEO had a higher miscibility coefficient value than the other mixtures. The neat polymers and mixtures were solution-blow-spun into nanofibers. The fiber diameters were smallest in the neat polymers. Transmission electron micrographs revealed a core/sheath structure for the sample mixtures. X-ray analysis indicated that the crystallinity was positively correlated with the PEO content. Fibers from the mixtures had contact angle measurements similar to those of the neat PEO. Fourier transform infrared and Raman spectroscopy of the mixtures indicated interactions between ester and ether groups, which were attributed to dipole–dipole interactions between the ester groups of PLA and the ether groups of PEO. © 2013 Wiley Periodicals, Inc. J. Appl. Polym. Sci. 129: 3672–3681, 2013

KEYWORDS: biofibers; biopolymers and renewable polymers; miscibility

Received 26 October 2011; accepted 5 January 2013; published online 2 March 2013

DOI: 10.1002/app.39061

INTRODUCTION

Polymers such as poly(lactic acid) (PLA) and poly(ethylene oxide) (PEO) have been explored in medical applications in many different forms, including films,[1,2] rods, microparticles and nanoparticles, and fiber mats.[3] Biodegradable nanoparticles have been widely studied because they can be used in injectable formulations,[4] oral products,[5] implants, and films.[1,2] Fiber mats using drug-loaded electrospun nanofibers have recently drawn a great deal of interest for applications in topical treatments, such as for malignant wounds and ulcers.[3] In comparison with other drug carriers, nanofibers have superior drug-encapsulation efficiency and structural stability.[3,6,7] Nanofiber mats are versatile in that they can be cut or fabricated to almost any size. Moreover, their porosity can be tailored through the control of the fiber diameter and mat thickness.

The properties of polymers used in controlled release devices may be engineered to improve drug-delivery profiles because the release rate may not necessarily coincide with the degradation rate of the polymer.[8,9] Several researchers have investigated the properties of stereocomplex crystallization between poly(L-lactide) (PLLA) and poly(D-lactide) (PDLA).[8,10,11] A higher crystallization increased the melting point, reduced the rate of hydrolysis, and provided longer sustained drug release compared to amorphous forms of PLA.[9,12–14] Modulated drug release has also been achieved with biodegradable amphiphilic block copolymers. Properties such as swelling, permeability, and degradation rate can be tailored by the segments selected for making block copolymers.[15] The hydrophobic segment is typically PLA or another biodegradable polyester, such as poly(glycolic acid).[15] The hydrophilic segment may be poly(ethylene glycol)

(PEG) because of its biocompatibility and solubility in both water and organic solvents.[15] PEO, which is simply a high-molecular-weight PEG (>20,000 g/mol), is also used extensively as the hydrophilic component of amphiphilic copolymers.[16]

The blending of polymers is another method of modifying the polymer properties. The advantage of blending polymers is the low cost, ease of preparation, and control of properties by the simple variation of the polymer ratios.[17,18] Blends of miscible polymers often are characterized by specific interactions, such as dipole–dipole, ion–dipole, and hydrogen-bonding interactions.[17,19] Information about these interactions can be measured to some extent by techniques in viscometry,[19–21] thermal and spectral analysis, and microscopy.[17,22]

The blending of hydrophilic and hydrophobic polymers is more challenging, but it has been used as yet another means of producing polymer devices for controlled release.[18] Such blends can provide a means of varying the hydration, degradation rate, and mechanical strength of controlled release devices. The dispersed-phase domains can serve as microreservoirs for drug loading in hydrophilic/hydrophobic polymer blends.[18,23,24] Microparticle blends of PLA and PEG were shown to be effective in the stabilization and controlled release of proteins.[24] PLA and PEG blends have provided controlled release of intranasal nanoparticle drug medication and in film coatings.[25,26] Nanofibers from emulsions containing PEO and an amphiphilic PEG–PLA diblock copolymer were produced by electrospinning. A core/sheath fiber morphology was formed, with the PEO component forming the core structure.[27] In yet another approach, blend polymer solutions of PLA and PEO were electrospun to produce fibers with enhanced hydrophilicity.[23] The fibers were highly porous with enhanced hydrophilicity, as measured by the contact angle.[23]

Recently, an alternative method, referred to as *solution blow spinning* (SBS), has been used to produce nanofibers in a way similar to that of electrospinning.[28] The SBS method uses a specialized nozzle and compressed gas, such as nitrogen, air, or argon, to form a structure similar to the Taylor's cone associated with the electrospinning process. In this technique, the fiber morphology can be controlled by both the solution variables (polymer concentration and viscosity, surface tension, evaporation rate, and polymer–solvent interaction parameters) and the process variables (working distance, spinning temperature, atmosphere used, spinning gas, and pressure).[28–31] SBS provides several advantages over the electrospinning process; these include safety, scalability, and versatility in solvent choice.[28] The objective of this study was to investigate the properties of PLA and PEO solvent mixtures and nanofibers with viscometry, microscopy, and thermal and spectral analyses.

Table I. Compositions of the Samples Studied

Sample	PLA/PEO polymer ratio	Mass fraction of PLA (wt %)
Neat PLA	1 : 0	100
Blend 1	3 : 1	75
Blend 2	1 : 1	50
Blend 3	1 : 3	25
Neat PEO	0 : 1	0

EXPERIMENTAL

Materials

PLA (number-average molecular weight = 75,000 g/mol) was obtained from Biomater (São Carlos, Brazil). PEO (number-average molecular weight = 100,000 g/mol) was obtained from Sigma-Aldrich. Chloroform ($CHCl_3$; CAS 67-66-3) and acetone [$(CH_3)_2CO$; CAS 67-64-1] were purchased from Synth Chemical (São Paulo, Brazil).

Methods

Five samples were tested; these included neat PLA, neat PEO, and three mixtures containing ratios of PLA to PEO of 3:1, 1:1, and 1:3 (Table I). For convenience, the five samples are also expressed on the basis of the PLA content (i.e., 100, 75, 50, 25, and 0 wt %; Table I). The samples were weighed and solvent-blended by dissolution in chloroform, as described later in greater detail.

Viscometry

Stock solutions of PLA and PEO (5 wt %) were prepared in chloroform. The viscosity measurements of each sample were performed in a suspended-level Ubbelohde capillary viscometer (Cannon, 50/F576) at 298 K. The efflux times of each sample were measured by serial dilution. A minimum of five dilutions were made for each sample. The specific viscosity (η_{sp}) was calculated at different concentrations from the efflux time measurements. A plot of η_{sp}/C against the solution concentration (C) for each blend composition was used to obtain the intrinsic viscosity ($[\eta]$) according to the following equation:

$$\eta_{sp}[n]C + K_H[\eta]^2C^2 \quad (1)$$

where K_H is the Huggins constant.[19,22] Finally, the miscibility coefficient (α) was calculated according to eq. (2) as per Sun et al.[21]

$$K_H = \frac{K_{PLA}[\eta_{PLA}]^2 w_{PLA}^2 + K_{PEO}[\eta_{PEO}]^2 w_{PEO}^2 + 2\sqrt{K_{PLA}K_{PEO}}[\eta_{PLA}][\eta_{PEO}]w_{PLA}w_{PEO}}{([\eta_{PLA}]w_{PLA} + [\eta_{PEO}]w_{PEO})^2} + \alpha \quad (2)$$

where K_H is the Huggins constant for a mixture and K_{PLA} and K_{PEO} are the Huggins constants for the pure polymer solutions of PLA and PEO, respectively. These values were 0.2, 1.6, 0.3, 0.5, and 0.8 for pure PLA, pure PEO, and blends 1, 2, and 3,

respectively (Table I). The ratios of PLA (w_{PLA}) and PEO (w_{PEO}) and the viscosities for the pure polymer solutions of PLA (η_{PLA}) and PEO (η_{PEO}) were used to determine K_H. The α parameter provided a measure of polymer–polymer interaction in the blends.[22,32]

Fiber Spinning by SBS

Five different samples, including neat PLA and PEO and the three mixtures (Table I), were prepared for SBS by carefully weighing of the appropriate amounts of dry polymer into test tubes. Chloroform was added to each test tube to bring the final polymer concentration to 6 wt %. The test tubes were rigorously stirred for several hours at room temperature to ensure complete dissolution. The polymer solutions were spun into nanofibers by SBS according to a method discussed by Medeiros et al.[28]. Briefly, the SBS apparatus consisted of a source of compressed air equipped with a pressure regulator, a glass syringe, and a syringe pump to control the injection rate of the polymer solutions. The spinning device consisted of a setup with concentric nozzles and a collector with a controllable rotation speed. A syringe pump (KD Scientific, model 781100, Holliston, USA) was used to feed the polymer solution (120 μL/min) through a central nozzle. Pressurized air was delivered through the concentric outer nozzle at a constant pressure (0.4 MPa). The inner nozzle was positioned so it protruded 2 mm beyond the concentric outer nozzle. The distance between the concentric nozzles was 0.5 mm, and the working distance was 12 cm. The SBS parameters were kept constant for all of the experiments. Nanofibers produced by SBS were collected on a rotating drum to produce nonwoven fiber mats. Fiber mats were collected for each of the five samples (Table I) and stored in a desiccator until they were needed for further analysis.

Microscopy

The morphology of the SBS fibers was analyzed with scanning electron microscopy (SEM; Zeiss, model DSM960, Jena, Germany). Samples were prepared by the cutting of fiber mats with a razor blade and their mounting on aluminum stubs with double-sided adhesive tape. The samples were then sputter-coated with gold (Balzers model SCD 050, Balzer Union AG, Balzers, Lichtenstein). The fiber diameters were measured with the aid of imaging software (Image J, National Institutes of Health). The average fiber diameter and size distribution were determined from approximately 100 random measurements with representative micrographs. Micrographs were also obtained with transmission electron microscopy (TEM; Tecnai G2 F20). Samples were prepared by the placement of a droplet of diluted aqueous fiber suspension on a carbon microgrid (400 mesh), and they were allowed to dry at room temperature. The images were acquired in TEM mode with a bright-field detector.

Contact Angle Measurements

The surface wettability was investigated by the measurement of the contact angle of a water droplet on the surface of the SBS fibers (nonwoven mats) with a contact angle meter (CAM 101 model, KSV Instruments, Ltd., Helsinki, Finland) equipped with a charge-coupled device camera (KGV-5000). In each measurement, a 5-μL droplet was pipetted onto the surface, and images of the droplet were automatically taken as a function of time. From these images, the contact angle values were calculated with dedicated software (KSV CAM2008). The measurements were carried out at 25°C and about 53% humidity.

Spectroscopy

Fourier transform infrared (FTIR) spectroscopy was performed with a Nicolet spectrometer (Nexus 470, Madison, WI). The FTIR spectrometer was purged continuously with nitrogen. A total of 64 scans were collected, with a resolution of 2 cm^{-1}. The IR spectra were recorded in transmission mode with thick films of solution-blow-spun polymer nanofibers, which were deposited on a silicon wafer.

Raman spectroscopy was used for comparison with X-ray diffraction (XRD) analyses. Data were recorded on a Fourier transform Raman spectrometer (RFS 100/S, Bruker, Inc., Karlsruhe, Germany) excited by an Nd:YAG laser at 1064 nm with a spectral resolution of 4 cm^{-1}.

XRD

Nonwoven fibrous mats produced by SBS were collected on aluminum foil and deposited on circular glass slides for analyses. XRD patterns were recorded with a Shimadzu (XRD-6000, Tokio, Japan) X-ray diffractometer. Scans were carried out from 10 to 30° [scattering angle (2θ)] at a scan rate of 2°/min with Ni-filtered Cu Kα radiation (wavelength = 0.154 nm at 50 kV and 20 mA). The full-width at half-maximum height (fwhm) of the diffraction peaks was calculated by the fitting of the XRD patterns with a Gaussian–Lorentzian function (Origin 7.5 software, Origin Lab, Northampton, USA). The d-spacing for a given 2θ was calculated by the application of the Bragg equation:

$$d = \frac{\lambda}{2 \sin \theta} \tag{3}$$

where λ is the wavelength of the Cu Kα radiation, θ is the Bragg angle.

The fwhm height (β; rad) of the diffraction peaks was calculated by the fitting of the XRD data with a Lorentzian function. The crystallite size (D) was estimated by calculation of the broadening of the diffraction peaks according to the Scherrer equation:

$$D = \frac{k\lambda}{\beta \sin \theta} \tag{4}$$

where k is the Scherrer constant and is dependent on the lattice direction and crystallite morphology. A k value of 0.9 was used in this study; this was based on values for these polymers found in the literature.[33,34] The fwhm of the diffraction peaks was calculated by the fitting of the XRD data with a Gaussian–Lorentzian function as per established methods.[35,36]

Thermal Analysis

Differential scanning calorimetry (DSC; TA Instruments calorimetric analyzer, model Q100, New Castle, USA) was performed under a nitrogen atmosphere at a flow rate of 20 mL/min and with a heating rate of 10°C/min. Samples were sealed in aluminum pans and heated from 0 to 180°C for PLA, −10 to 120°C for PEO, and −10 to 180°C for the blends of PLA and PEO.

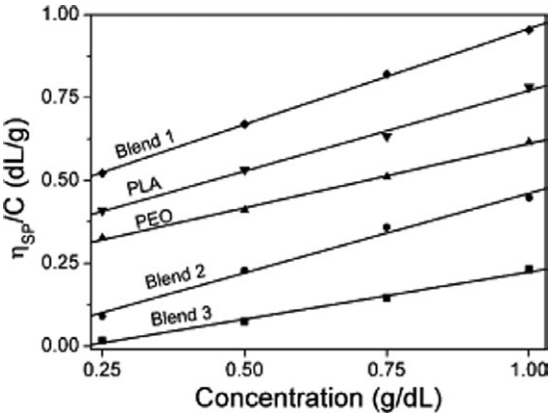

Figure 1. η_{sp} versus concentration plot for the neat polymers and blends.

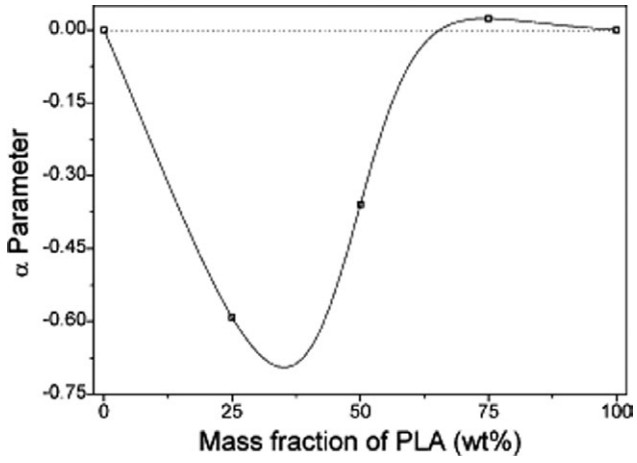

Figure 2. Viscometric parameter (α) calculated for five samples, including the neat polymers of PLA and PEO and three polymer mixtures.

RESULTS AND DISCUSSION

Viscometry

Dilute solution viscometry is one of the least expensive and most simple ways to determine the polymer miscibility.[17] Dilute solution viscometry makes the reasonable assumption that if molecules are attractive in dilute solution, they most likely interact in bulk and have some degree of miscibility.[17,21] Sun et al.[21] derived a miscibility coefficient (α) from the classical Huggins constant; it is also known as the α parameter and is a measure of the degree of interaction between two polymers in a blend.

According to Sun et al.,[21] the Huggins constant arise from hydrodynamic and thermodynamic interactions between two polymers. Intramolecular and intermolecular effects associated with the excluded volume are also considered. The Huggins parameter, however, takes into account only interactions between chain segments under the action of shear forces, whereas the α parameter considers that if specific interactions occur between chains in dilute solutions, a similar behavior will occur in the solid state.

Sun et al.[21] also found that polymers were miscible when their α values were greater than or equal to zero and immiscible when their α values were negative.[21] This was directly correlated with the repulsive ($\alpha < 0$) and attractive ($\alpha \geq 0$) forces, respectively, between the molecules in dilute solutions.

From viscometry measurements of dilute solvent blends plotted against the mass fraction of PLA (Figure 1) and eqs. (1) and (2), α values were obtained for the polymers and blends (Figure 2). The α parameter was near zero as expected for the neat polymer solutions of PLA and PEO. Blends of 1:1 and 1:3 PLA/PEO gave negative α values; this indicated immiscibility (Figure 2). Surprisingly, the α value for the 3:1 PLA/PEO blend was also greater than zero; this indicated miscibility.

The immiscibility of the PLA/PEO blends was studied previously by Gaikwad et al.,[37] who observed that the presence of two separate glass transitions was not necessarily indicative of polymer immiscibility. They studied a full range of PLA/PEO blends and observed a broadening of the glass transition width compared to the neat polymer and changes in the crystallinity of PEO, all of which were indicative of polymer–polymer interactions. Bognitzki et al.[38] studied the morphology of immiscible blends of PLA and poly(vinyl pyrrolidone). Their objective was to preserve the cocontinuous or interpenetrating phase morphologies initially present in a blend by instantaneously freezing the structure using the electrospinning process for forming fibers. In a manner similar to electrospinning, the SBS process exhibited very fast solvent evaporation and polymer solidification; this may have reduced the phase separation and improved the polymer compatibility. The mechanisms of phase separation during the solvent evaporation of immiscible polymer blends (in the solid state) prepared from miscible solutions have already been reported in the literature for several blends.[39,40]

SEM

The SBS process was effective in producing nonwoven mats of nanofibers from polymer solutions of the blends and the neat polymers (Figure 3). In contrast to the porous fiber morphology reported earlier for PLA/PEO blends,[23] the fibers from this study were generally smooth and nonporous (Figure 3). This was most likely due to the lower vapor pressure of chloroform used in this study.[23] The fibers from polymer solutions of PLA and PEO [Figure 3(a,e)] were smooth and had smaller average diameters than the fibers made from polymer mixtures (Figure 4). The variability of the fiber diameter was lower for neat PEO than for neat PLA (Figure 4). Even though some PEO fiber samples exhibited some variability in the fiber diameter [Figure 3(e)], the overall variability was lower; this was most likely due to the differences in the rheological properties of the two polymers.

The fibers from the 3:1 PLA/PEO blend [Figure 3(b)] were also smooth. In contrast, fibers made from the 1:1 and 1:3 PLA/PEO mixtures had particles deposited on the fiber surface (Figure 3). Many of the particles were in the submicrometer range [Figure 3(c,d)]. The formation of the particles could have been related to the increased concentration of each polymer as the solvent evaporated. The least soluble polymer may have begun to salt out and increase the viscosity of the blend; this could explain the thicker fibers.

Applied Polymer SCIENCE

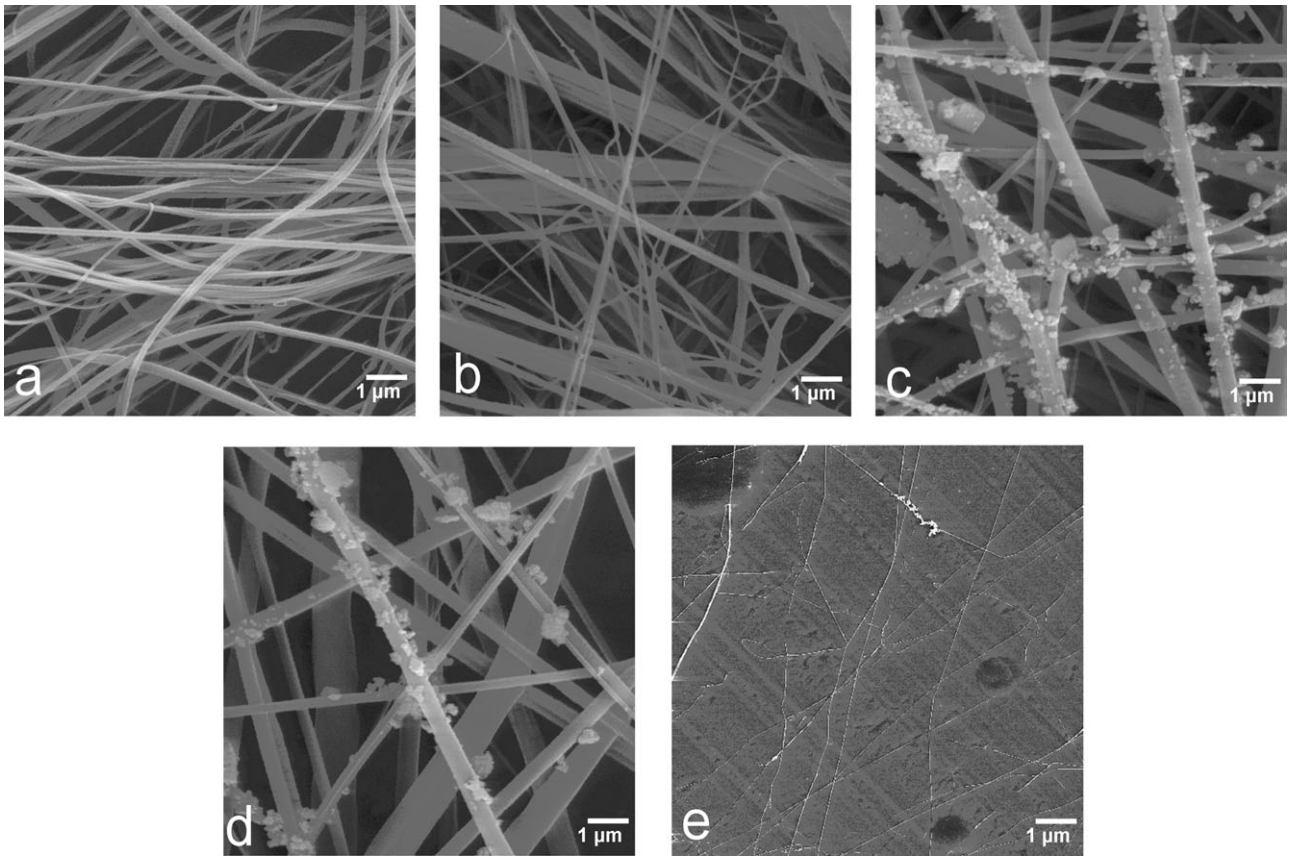

Figure 3. Scanning electron micrographs of the solution-blow spun nanofibers of (a) neat PLA, (b) a 3:1 mixture of PLA and PEO, (c) a 1:1 mixture of PLA and PEO, (d) a 1:3 mixture of PLA and PEO, and (e) neat PEO.

As mentioned previously, the diameter of fibers made from the neat polymer was smaller than the fiber diameter made from the polymer mixtures; this was consistent with polymer mixtures having poor compatibility (Figure 4). However, the 3:1 PLA/PEO mixture (Figure 4, 75 wt %) had a more consistent fiber diameter (lower standard deviation) than the other mixtures and did not form particles on the fiber surface [Figure 3(b)]. Blend 1 exhibited a more homogeneous morphology than other mixtures because of its rheological properties.

Contact Angle Measurements

The contact angle data provided evidence that some fraction of the PEO was exposed on the fiber surface in all of the blends tested (Figure 5). The fibers of neat PLA and PEO had contact angles of 120 and 38°, respectively. The contact angle for all of the fiber blends was within the range of the neat PEO sample

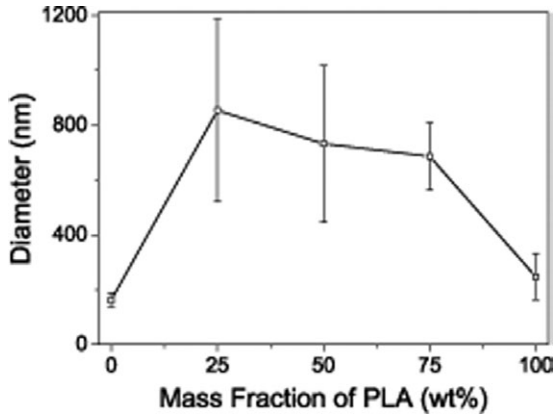

Figure 4. Fiber diameters (in nanometers) of the neat PLA (100%), neat PEO (0%), and three blends of PLA and PEO. The error bars indicate the standard deviation.

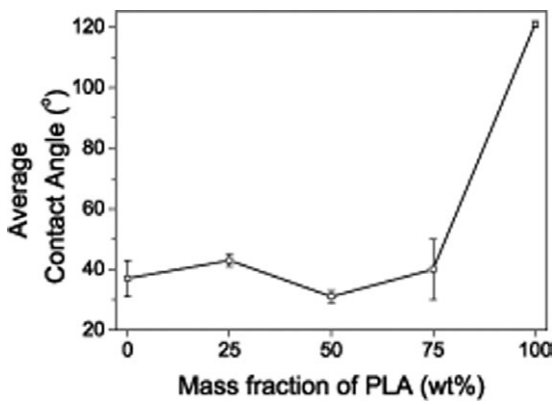

Figure 5. Contact angle measurements made on the nonwoven fiber mats of the neat PLA (100%), neat PEO (0%), and three blends of PLA and PEO. The error bars indicate the standard deviation.

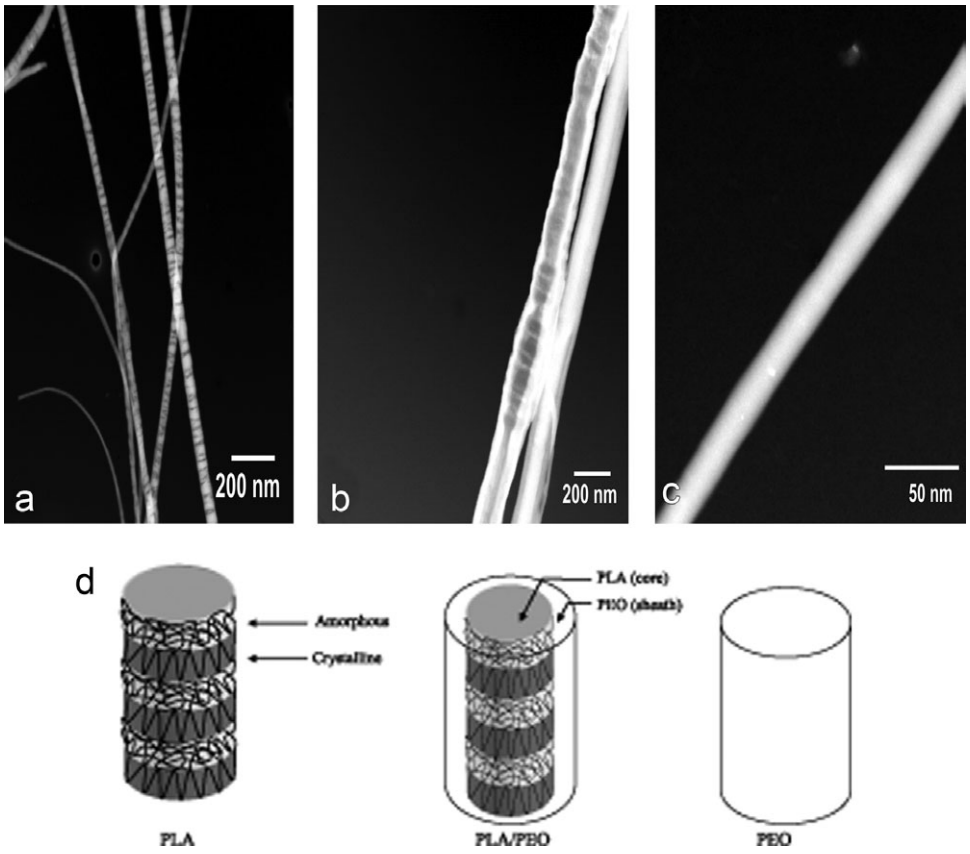

Figure 6. TEM images of nanofibers from the (a) neat PLA, (b) 1 : 1 blend of PLA and PEO, and (c) neat PEO and (d) schematic depiction of the structural development in the fibers.

(Figure 5). There was no significant difference in the contact angle values between the blends and the PEO samples. Even the 3:1 blend of PLA and PEO had a low contact angle. These results indicate that some fraction of PEO was exposed on the fiber surface in each of the blends, including the 3:1 blend. With the knowledge that one-third of the bulk material was PEO, we determined that there was about the same amount of PEO on the surface of the fibers. Therefore, when a water droplet was in contact with the fiber surface, the PEO fraction may have also absorbed water from the droplet, with an overall effect of changing the contact angle values.

TEM

The TEM micrographs provided evidence that fibers made from the polymer mixtures were comprised of core/sheath structures with PLA in the core and PEO in the sheath. Neat PLA fibers showed a bamboolike structure [Figure 6(a)]; this was similar to previous reports, in which PLA was comprised of a striated structure with crystalline regions of about 20 nm in length and amorphous phases of about 6 nm.[41] In contrast to the neat PLA fibers, the neat PEO fibers appeared homogeneous with no distinctive microstructure [Figure 6(c)].

The fibers made from a 1:1 mixture of PLA and PEO formed a core/sheath matrix; this indicated that the core was comprised of one polymer and the sheath was comprised of the other [Figure 6(b)]. The sheath structure of the fibers was most likely comprised of PEO because it did not have the striated appearance that is common to PLA fibers [Figure 6(a)]. The contact angle data was consistent, with the sheath being comprised of PEO (Figure 5). A sheath comprised of PEO would, by default, indicate that the core structure was comprised of PLA. Evidence for a PLA core was found in some fibers, where the core exhibited a striated pattern similar to that of the neat PLA fibers [Figure 6(a)]. It was not clear why the striated pattern in the fiber core was not visible in all of the fibers [Figure 6(b)]. Nevertheless, all fibers made from the 1:1 mixture of PLA and PEO should have had the same core/sheath structure, and the contact angle data supported the evidence that the sheath was comprised of PEO.

Core/sheath structures, which were formed due to a combination of several factors, such as differences in the surface tension, polymer–solvent, and polymer–polymer interactions, have been reported previously for blends of PEO and an amphiphilic copolymer (PEG–PLA) blended in an oil/water emulsion.[27] The emulsion was electrospun to form nanofibers with a PEO core and a PEG–PLA copolymer sheath. Evidence of the core/sheath structure was not observed in the 3:1 PLA/PEO fiber samples (data not shown). However, because the contact angle measurements for the 3:1 mixture was similar to that of the neat PEO sample, it was reasonable to conclude that a significant fraction of the PEO was exposed on the fiber surface, even when a clear core/sheath structure was not formed.

Applied Polymer SCIENCE

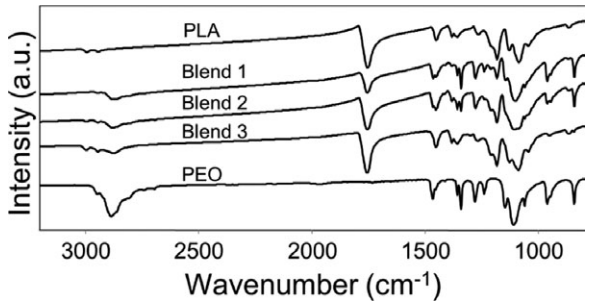

Figure 7. FTIR spectra of fibers from the neat PLA, blend 1 (1 : 3 PLA/PEO), blend 2 (1 : 1 PLA/PEO), blend 3 (1 : 3 PLA/PEO), and neat PEO.

Spectroscopy

Immiscible blends may become single-phase blends if low levels of hydrogen bonding can be introduced.[42] Among spectroscopic techniques, including NMR and fluorescence, IR spectroscopy is particularly useful in analyzing chemical interaction. The spectral band width and intensity may be correlated with the strength and extent of hydrogen bonding.[42] Two completely incompatible polymers show no spectral interaction, whereas compatible polymers that have chemical interactions will reflect such changes in the IR spectrum in the form of band shifts, band widening, and changes in the band intensity.[42–46] The IR spectra (600–3200-cm^{-1} region) of the PLA/PEO mixtures were consistent with chemical interactions between PLA and PEO (Figure 7).

The relative intensity of the carbonyl band (COC) in PLA decreased, and this was observed in the spectra of all of the blends (Table II). This decrease reflected the new distribution of the 3_1 helix of PLA, which resulted from the competition between ester and ether groups in the polymer blends. The structure of the α crystal of PLA was pseudo-orthorhombic with the chains in $-10/3$ helical and $-3/1$ helical conformations for the β crystals.[47] A triclinic unit cell for the PLA stereocomplex consisting of PLLA and PDLA chains in a 3_1 helical conformation (three monomers per turn) was reported in the literature.[45] The relative intensity of the ether band (CO) in PEO increased, and it was also observed in the spectra of all of the blends (Table II). This increase also explained the new distribution of a helical conformation of PEO, which resulted from competition between the ester and ether groups in the polymer blends (Table II). The relative intensity between the ester band (C=O) and ether band (CO) was highest for blend 1, equal for blend 2, and lowest for blend 3 (Table II); this indicated that there were more interactions between the ester and ether groups of blend 1 and that these interactions gradually decreased with decreasing PLA content (Table II).

Table II. FTIR Band Ratio

Assignment	Wave numbers	PLA	Blend 1	Blend 2	Blend 3	PEO
COC/CH_3	1092/1456	0.5	0.3	0.2	0.4	—
CO/CH_2	1110/2886	—	0.9	0.8	0.7	0.6
C=O/CO	1755/1110	—	2.5	1.1	0.8	—

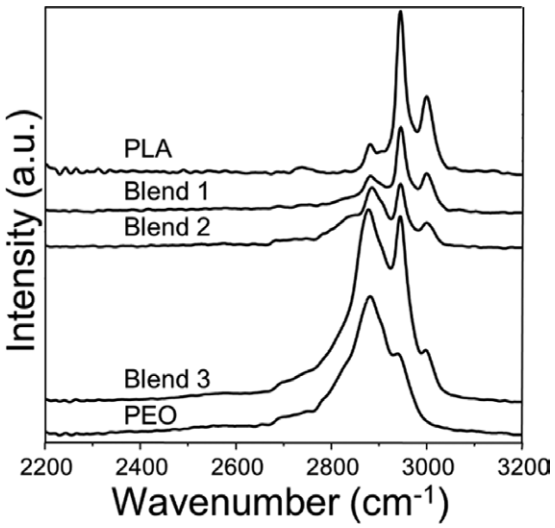

Figure 8. Raman spectra of fibers from the neat PLA, blend 1 (1 : 3 PLA/PEO), blend 2 (1 : 1 PLA/PEO), blend 3 (1 : 3 PLA/PEO), and neat PEO.

The band at 873 cm^{-1} could be assigned to the stretching mode of νC—COO in PLA (Figure 8) in accordance with previous work.[45,48] The bands at 843 and 803 cm^{-1} could, therefore, be assigned to the C—C stretching and CH_2 rocking in skeleton vibrations in PEO (Figure 8).[49]

The relative intensities of the νC—COO (PLA)/skeleton vibrations (PEO) was 5.0 for blend 1 and 1.0 for blends 2 and 3, and this was observed in the Raman spectrum (Figure 8). This result was consistent with the FTIR data and indicated there were more interactions between the ester and ether groups in blend 1 than in blends 2 and 3. The strong interactions between the ester and ether groups could have accounted for the apparent miscibility in blend 1.

XRD

XRD was carried out to determine the crystal structure in the solution-blow-spun polymeric fibers. The diffraction patterns (Figure 9) showed that the blends had some peaks in common with the neat polymers. A comparison in terms of crystallinity, *d*-spacing, and *D* was also carried out and is summarized in Table III. The samples clearly exhibited two reflection peaks (near 13 and 16°), ascribed to α crystals, and a small peak (near 24.8°) associated with the β phase.[7,47] The formation of β crystals was caused by the different extents of deformation of the polymer molecules during fiber formation by SBS.[7] PLA fibers had a crystallinity of 71% according to the Lorentzian fit (Table III).

The XRD patterns of the PEO fibers indicated that PEO was a semicrystalline polymer with diffraction peaks at $2\theta = 19$ and 23°[50]. Distinct peaks characteristic of PEO crystallites ($2\theta = 14$, 17, and 25.4°) were observed (Table III); these indicated that solvent-induced polymer crystallization occurred. The increase in the percentage of PEO in the mixtures led to an increase in crystallinity. The size of the PLA crystallite (24.8°) increased with higher amounts of PEO (Table III). The results provided evidence that the nucleation and growth step of crystallization in PLA was controlled by the interaction of polymers in the

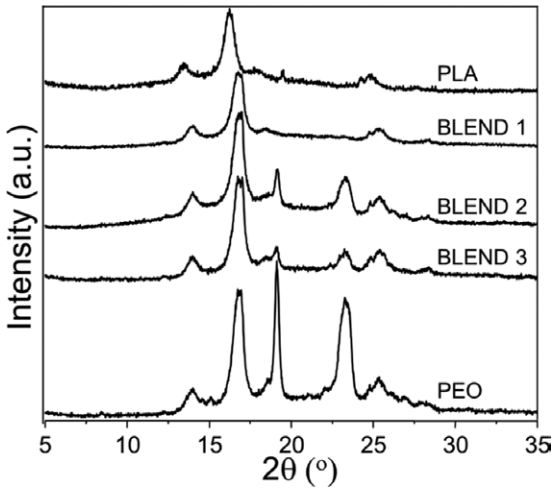

Figure 9. XRD patterns for the neat polymers and blends.

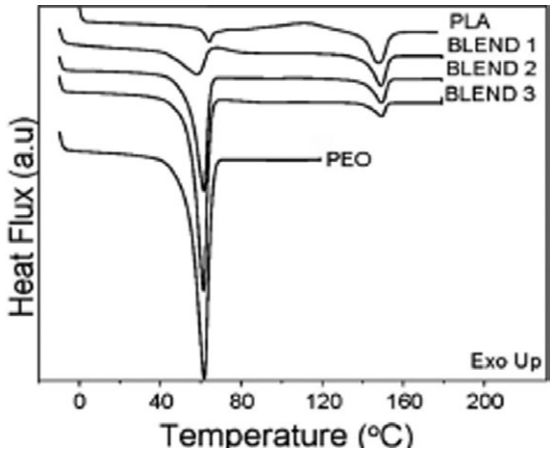

Figure 10. Thermograms from DSC scans of the neat PLA, neat PEO, and blends. The blends consisted of ratios of 3 : 1 (blend 1), 1 : 1 (blend 2), and 1 : 3 (blend 3) of PLA and PEO.

mixtures during fiber formation by SBS. These results could have relevance for controlled drug delivery because D was used to control drug release in the fibers.[51] Moreover, the crystallinity impacted not only the mechanical strength of the mats but also the rate of polymer degradation and absorption in biological environments. This might have been due to the simultaneous crystallization of the PLA and PEO chains. Because the two neat polymers formed crystals whose unit cells had different parameters (a, b, and c axis), during the simultaneous crystallization of the PLA/PEO chains, one polymer, say PLA, could become entangled with PEO chains and vice versa, and this would give rise to more imperfect unit cells (larger crystals). Moreover, the degree of immiscibility (phase separation) might have significantly contributed to the alteration of the cell parameters (perfection) and, thus, the crystallinity.

Thermal Analysis

DSC is generally one of the most convenient methods for analyzing first-order transitions such as melting and crystallization. DSC curves were obtained for each of the fiber samples (Figure 10).

The DSC data was used to determine the heat of fusion (ΔH_f) and melting temperature (T_m) for both PEO and PLA [Figure 11(a,b)]. The presence of two intense melting peaks indicated the semicrystalline nature of the PEO (62.4°C) and PLA [147.7°C; Figure 11(a,b)] and, therefore, corroborated the XRD data. Values of ΔH_f were calculated by the integration of the area under the endothermic curves for fibers of PEO without and with PLA. We found that the PEO melting point and ΔH_f (percentage crystallinity) decreased linearly as the PLA content increased in the fiber blends. The decrease in PEO ΔH_f [Figure

Table III. Crystallization Parameters of the Fibers

System	Crystallinity of the mats (%)	PLA crystallite (24.8°)		PEO crystallite (25.4°)	
		d-spacing (Å)	*D* (Å)	*d*-spacing (Å)	*D* (Å)
Neat PLA	71	3.6	0.9	—	—
Blend 1	51	3.6	7.4	3.5	1.7
Blend 2	79	3.6	10.3	3.5	1.9
Blend 3	87	3.6	4.6	3.5	1.6
Neat PEO	93	—	—	3.5	1.6

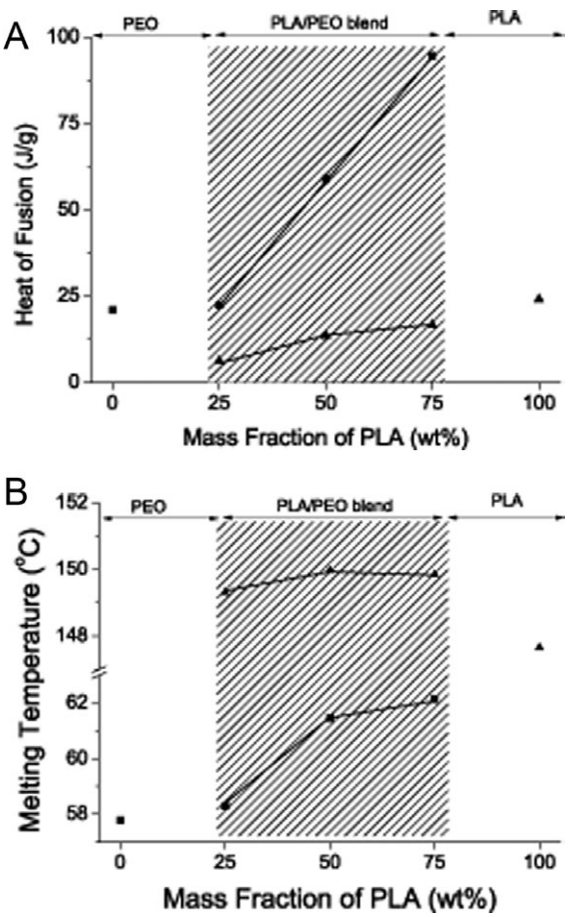

Figure 11. (a) ΔH_f and (b) T_m of PEO, PLA, and the PLA/PEO blends.

11(a)] with the addition of PLA could be explained either by a decrease in the rate of crystallization or by blockage of the crystalline growth front caused by the PLA crystallites dispersed in an irregular array in the fiber blend, as evident from spectroscopy and microscopy studies. The increase in the PLA ΔH_f and T_m values [Figure 11(b)] in the blend fibers was attributed to the fact that the PLA crystallites in the blends were larger than in neat PLA. This explanation was consistent with XRD results.

CONCLUSIONS

The interaction of PLA and PEO are of broad interest, partly because of the wide use of these polymers in medical applications. The modification of the properties of these polymers through solution blending has the potential to create new applications. Although PLA and PEO are generally regarded as immiscible, the results of this study indicate that the polymers do interact differently when they are solution blended, depending on the ratios of the blends. The degree of polymer interaction was highest in the 3:1 PLA:PEO blend. Polymer interaction was confirmed by viscometry and various thermal and spectroscopic methods. The nature of the interaction was most likely a result of dipole–dipole interactions between the ester groups of PLA and the ether groups of the PEO.

ACKNOWLEDGMENTS

The authors thank Agencia financiadora de estudos e projetos (FINEP)/Ministério da Ciência e Tecnologia (MCT), Conselho Nacional de Desenvolvimento Científico e Tecnolœgico (CNPq), Coordenação de Aperfeiçoamento de Pessoal de Nível Superior (CAPES), Embrapa/Laboratório Nacional de Nanotecnologia aplicada ao Agronegócio (LNNA), and Fundação de Pesquisa do Estado de São Paulo (FAPES) for their financial support.

REFERENCES

1. Kim, D.-H.; Martin, D. C. *Biomaterials* **2006**, *27*, 3031.
2. Galeska, I.; Kim, T.-K.; Patil, S.; Bhardwaj, U.; Chatttopadhyay, D.; Papadimitrakopoulos, F.; Burgess, D. *AAPS J.* **2005**, *7*, E231.
3. Xu, X.; Zhong, W.; Zhou, S.; Trajtman, A.; Alfa, M. *J. Appl. Polym. Sci.* **2010**, *118*, 588.
4. Wischke, C.; Schwendeman, S. P. *Int. J. Pharm.* **2008**, *364*, 298.
5. des Rieux, A.; Fievez, V.; Garinot, M.; Schneider, Y.-J.; Préat, V. *J. Controlled Release* **2006**, *116*, 1.
6. Kumbar, S. G.; Nair, L. S.; Bhattacharyya, S.; Laurencin, C. T. *J. Nanosci. Nanotechnol.* **2006**, *6*, 2591.
7. Zhou, H.; Green, T. B.; Joo, Y. *L. Polymer* **2006**, *47*, 7497.
8. Tsuji, H.; Tezuka, Y. *Biomacromolecules* **2004**, *5*, 1181.
9. Ishii, D.; Ying, T. H.; Mahara, A.; Murakami, S.; Yamaoka, T.; Lee, W.-K.; Iwata, T. *Biomacromolecules* **2008**, *10*, 237.
10. Tsuji, H. *Biomaterials* **2003**, *24*, 537.
11. Fukushima, K.; Kimura, Y. *Polym. Int.* **2006**, *55*, 626.
12. Slager, J.; Domb, A. *J. Biomacromolecules* **2003**, *4*, 1316.
13. Slivniak, R.; Domb, A. *J. Biomacromolecules* **2002**, *3*, 754.
14. Brannon-Peppas, L. *Int. J. Pharm.* **1995**, *116*, 1.
15. Bezemer, J. M.; Radersma, R.; Grijpma, D. W.; Dijkstra, P. J.; van Blitterswijk, C. A.; Feijen, J. *J. Controlled Release* **2000**, *67*, 249.
16. Uhrich, K. E.; Cannizzaro, S. M.; Langer, R. S.; Shakesheff, K. M. *Chem. Rev.* **1999**, *99*, 3181.
17. Parashar, P.; Ramakrishna, K.; Ramaprasad, A. T. *J. Appl. Polym. Sci.* **2011**, *120*, 1729.
18. Bajpai, A. K.; Shukla, S. K.; Bhanu, S.; Kankane, S. *Prog. Polym. Sci.* **2008**, *33*, 1088.
19. Lizymol, P. P.; Thomas, S. *Eur. Polym. J.* **1994**, *30*, 1135.
20. Chee, K. *K. Eur. Polym. J.* **1990**, *26*, 423.
21. Sun, Z.; Wang, W.; Feng, Z. *Eur. Polym. J.* **1992**, *28*, 1259.
22. Akhlaghi, S.; Sharif, A.; Kalaee, M.; Manafi, M. *J. Appl. Polym. Sci.* **2011**, *121*, 3252.
23. Honarbakhsh, S.; Pourdeyhimi, B. *J. Mater. Sci.* **2011**, *46*, 2874.
24. Jiang, W.; Schwendeman, S. P. *Pharm. Res.* **2001**, *18*, 878.
25. Mainardes, R. M.; Khalil, N. M.; Gremião, M. P. D. *Int. J. Pharm.* **2010**, *395*, 266.
26. Liu,X.; Lei,L.; Hou,J.-W.; Tang,M.-F.; Guo,S.-R.; Wang,Z.-M.; Chen,K.-M. *J. Mater. Sci. Mater. Med.* **2011**, *22*, 327.
27. Xu, X.; Zhuang, X.; Chen, X.; Wang, X.; Yang, L.; Jing, X. *Macromol. Rapid Commun.* **2006**, *27*, 1637.
28. Medeiros, E. S.; Glenn, G. M.; Klamczynski, A. P.; Orts, W. J.; Mattoso, L. H. C. *J. Appl. Polym. Sci.* **2009**, *113*, 2322.
29. Oliveira, J. E.; Mattoso, L. H. C.; Medeiros, E. S.; Zucolotto, V. *Biosensors* **2012**, *2*, 70.
30. Oliveira, J. E.; Moraes, E. A.; Costa, R. G. F.; Afonso, A. S.; Mattoso, L. H. C.; Orts, W. J.; Medeiros, E. S. *J. Appl. Polym. Sci.* **2011**, *122*, 3396.
31. Oliveira, J. E.; Zucolotto, V.; Mattoso, L. H. C.; Medeiros, E. S. *J. Nanosci. Nanotechnol.* **2012**, *12*, 2733.
32. da Silva Neiro, S. M.; Dragunski, D. C.; Rubira, A. F.; Muniz, E. C. *Eur. Polym. J.* **2000**, *36*, 583.
33. Huang, P.; Zheng, J. X.; Leng, S.; Van Horn, R. M.; Jeong, K.-U.; Guo, Y.; Quirk, R. P.; Cheng, S. Z. D.; Lotz, B.; Thomas, E. L.; Hsiao, B. S. *Macromolecules* **2007**, *40*, 526.
34. Marega, C.; Marigo, A.; Di Noto, V.; Zannetti, R.; Martorana, A.; Paganetto, G. *Makromol. Chem.* **1992**, *193*, 1599.
35. Khayet, M.; García-Payo, M. C. *Desalination* **2009**, *245*, 494.
36. Bhattacharyya, A. R.; Sreekumar, T. V.; Liu, T.; Kumar, S.; Ericson, L. M.; Hauge, R. H.; Smalley, R. E. *Polymer* **2003**, *44*, 2373.
37. Gaikwad, A. N.; Wood, E. R.; Ngai, T.; Lodge, T. P. *Macromolecules* **2008**, *41*, 2502.
38. Bognitzki, M.; Frese, T.; Steinhart, M.; Greiner, A.; Wendorff, J. H.; Schaper, A.; Hellwig, M. *Polym. Eng. Sci.* **2001**, *41*, 982.
39. Kano, Y.; Sato, H.; Okamoto, M.; Kotaka, T.; Akiyama, S. *J. Adhes. Sci. Technol.* **1999**, *13*, 1243.
40. Liu, T.; Ozisik, R.; Siegel, R. W. *Thin Solid Films* **2007**, *515*, 2965.

41. Picciochi, R.; Wang, Y.; Alves, N. l.; Mano, J. O. *Colloid Polym. Sci.* **2007**, *285*, 575.
42. Dong, J.; Ozaki, Y. *Macromolecules* **1997**, *30*, 286.
43. Angood, A. C.; Koenig, J. L. *J. Appl. Phys.* **1968**, *39*, 4985.
44. Kang, S.; Hsu, S. L.; Stidham, H. D.; Smith, P. B.; Leugers, M. A.; Yang, X. *Macromolecules* **2001**, *34*, 4542.
45. Kister, G.; Cassanas, G.; Vert, M. *Polymer* **1998**, *39*, 267.
46. Miyazawa, T.; Fukushima, K.; Ideguchi, Y. *J. Chem. Phys.* **1962**, *37*, 2764.
47. Hoogsteen, W.; Postema, A. R.; Pennings, A. J.; Ten Brinke,G.; Zugenmaier,P. *Macromolecules* **1990**, *23*, 634.
48. Yang, X.; Kang, S.; Hsu, S. L.; Stidham, H. D.; Smith, P. B.; Leugers, A. *Macromolecules* **2001**, *34*, 5037.
49. Kozielski, M.; Muhle, M.; Blaszczak, Z. A. *J. Mol. Liq.* **2004**, *111*, 1.
50. Davison,W. H. T. *J. Chem. Soc.* **1955**, 3270.
51. Freiberg, S.; Zhu, X. *X. Int. J. Pharm.* **2004**, *282*, 1.